Review of Scientific Instruments

RESEARCH ARTICLE | APRIL 21 2026

High-pressure generation above 45 GPa over a 10 mm³ volume with a multi-anvil press

Guoliang Niu ; Lianjie Man ; Peiyang Mu; Junkai Li; Rémy Pierru; Amrita Chakraborti ; Shuai Tang ; Cheng Qian; Shengbo Cao ; Shijing Zhao ; Bingmin Yan; Robert Farla ; Chunyin Zhou ; Xiaokang Feng; Youwen Long ; Ke Yang; Kui Han ; Huiyang Gou

Rev. Sci. Instrum. 97, 043903 (2026)
https://doi.org/10.1063/5.0323039

Review of Scientific Instruments ARTICLE pubs.aip.org/aip/rsi

High-pressure generation above 45 GPa over a 10 mm³ volume with a multi-anvil press

Cite as: Rev. Sci. Instrum. 97, 043903 (2026); doi: 10.1063/5.0323039
Submitted: 15 January 2026 • Accepted: 28 March 2026 •
Published Online: 21 April 2026

Guoliang Niu,[1] Lianjie Man,[2,a)] Peiyang Mu,[1] Junkai Li,[1] Rémy Pierru,[2] Amrita Chakraborti,[2] Shuai Tang,[3] Cheng Qian,[2] Shengbo Cao,[1] Shijing Zhao,[1] Bingmin Yan,[1] Robert Farla,[4] Chunyin Zhou,[5] Xiaokang Feng,[4] Youwen Long,[3] Ke Yang,[5] Kui Han,[6] and Huiyang Gou[1,b)]

AFFILIATIONS

[1] Center for High Pressure Science and Technology Advanced Research, Beijing 100193, China
[2] Bayerisches Geoinstitut, University of Bayreuth, 95440 Bayreuth, Germany
[3] Beijing National Laboratory for Condensed Matter Physics, Institute of Physics, Chinese Academy of Sciences, Beijing 100190, China
[4] Deutsches Elektronen-Synchrotron DESY, Notkestraße 85, 22607 Hamburg, Germany
[5] Shanghai Advanced Research Institute, Chinese Academy of Sciences, Shanghai 201210, China
[6] Key Laboratory of Earth Exploration and Information Techniques, College of Geophysics, Chengdu University of Technology, 610059 Chengdu, China

[a)] **Current address:** Institute of Geochemistry and Petrology, ETH Zürich, Sonneggstrasse 5, CH-8092 Zürich, Switzerland.
[b)] **Author to whom correspondence should be addressed:** huiyang.gou@hpstar.ac.cn

ABSTRACT

High-pressure generation in multi-anvil presses has long been limited to pressures below ~25 GPa when millimeter-scale samples are required. In this study, we systematically optimized the experimental setup for a Kawai-cell assembly using tungsten carbide anvils with a truncation edge length (TEL) of 3 mm to extend the achievable pressure range. Our results show that, in contrast to previous studies using smaller assemblies (TEL = 1.5 and 1.0 mm), tapering the anvils solely has a negligible effect on pressure-generation capability for the large sample volumes investigated here, despite a substantial increase in anvil gap under the same load. In contrast, reducing the gasket volume significantly improves the efficiency of press-load transmission to the sample, enabling an ~33% increase in pressure compared with conventional designs using the same type of anvil. Using the optimized gasket design together with ultrahard tungsten carbide anvils with a 1° taper (TJS01, Fujilloy; TEL = 3 mm), pressures of up to 45.8 GPa were achieved at room temperature while maintaining a truncation-confined volume >10 mm^3 and an anvil gap >0.3 mm. This technical breakthrough not only enables the synthesis of functional materials with large sample volumes at pressures above 45 GPa but also opens doors to unprecedentedly high pressures for precise physical property measurements that require large sample volumes and large anvil gaps, including ultrasonic interferometry, electrical impedance, and thermal conductivity measurements in a multi-anvil press.

I. INTRODUCTION

The multi-anvil press is a widely used device for generating high-pressure and high-temperature (HP–HT) conditions in geoscience and materials science.[1–4] By employing second-stage anvils consisting of eight tungsten carbide (WC) anvils with truncated corners that compress an octahedral assembly ("6–8 type"), the Kawai-type multi-anvil assembly has conventionally been used to generate pressures up to ~25 GPa.[5] Compared to another popular static compression technique, the diamond anvil cell (DAC), the multi-anvil press typically offers sample volumes that are a few orders of magnitude larger and also provides more homogeneous P–T fields.[6] So, this enables precise *in situ* measurements of physical properties on bulk samples under high-pressure and high-temperature (HP–HT) conditions.[7–9] However, a major limitation of the multi-anvil technique is its limited pressure-generation capability, which remains far below that of diamond anvil cells (DACs); the latter can generate pressures up to ~1 TPa,[10] although with severely

limited sample volumes (tens to hundreds of μm^3), in contrast to the much larger volumes attainable in conventional multi-anvil experiments (tens to hundreds of mm^3). This technical limitation of the multi-anvil technique has hindered the exploration of a range of fundamental scientific questions. For example, direct measurements of the shear and bulk moduli of mantle minerals under lower-mantle conditions (up to ~135 GPa) are required to correctly interpret seismic observations and to constrain the composition of the bulk silicate Earth (e.g., Ref. 11). However, such experiments remain elusive with conventional multi-anvil setups.

Recent advancements in multi-anvil techniques include optimizing the geometry of second-stage anvils[12,13] and employing ultrahard, although expensive, anvils, such as C2-grade sintered diamond (SD) anvils[14] from Sumitomo and TJS01 tungsten carbide anvils from Fujilloy,[12,15] which together have enabled pressure generation approaching[16] or exceeding 100 GPa.[13,14] However, these extremely high pressures are achieved at the expense of sample volume: the use of anvils with reduced TELs (e.g., 1.5 or 1.0 mm) results in significantly reduced truncation-confined volumes, which are ~87.5% and ~96.3% smaller than those obtained using the conventional multi-anvil assemblies with a TEL of 3 mm, respectively. Such small anvils defeat the primary advantage of the multi-anvil technique, making it difficult to obtain a sufficiently large sample for post-characterization such as Vickers hardness testing, single-crystal X-ray diffraction, or comprehensive measurements of other properties. More critically, *in situ* measurements of bulk physical properties under HP–HT conditions are nearly impossible with such a small sample volume. Another approach to increasing the pressure-generation capability of multi-anvil presses is the introduction of a third-stage anvil (6–8–2 configuration), in which diamond anvils/pistons are embedded within the octahedral pressure medium.[17–19] Using this configuration, pressures of up to ~125 GPa at room temperature have been achieved.[17] However, large differential stresses are expected within the sample under such highly uniaxial compression conditions, which do not satisfy the quasi-hydrostatic requirements of most high-pressure studies. In addition, the effective sample volume at peak pressure is confined to a small region near the center of the diamond anvils/pistons, similar to that in DAC experiments.[20] This volume is, therefore, substantially smaller than that attainable in conventional 6–8 multi-anvil experiments, where pressure can be maintained relatively homogeneously over a large region within the octahedral pressure medium.

In this study, we systematically optimized the pressure-generation capability of a 7/3 Kawai-type assembly [7 mm octahedral edge length (OEL) and 3 mm truncation edge length (TEL)] to extend the achievable pressure range in a multi-anvil press, while maintaining a sufficiently large sample volume for *ex situ* characterization and *in situ* bulk physical property measurements. The primary objective is to extend the pressure range of conventional 3 mm TEL assemblies without sacrificing sample volume or anvil gap. This was achieved through a set of synergistic strategies, including the optimization of the gasket geometry, the use of tapered anvils, and the application of ultrahard WC anvils (TJS01). As a result, pressures of up to 45.8 GPa were achieved at room temperature while preserving an anvil gap exceeding 0.3 mm, demonstrating a significant extension of the pressure range accessible to large-volume multi-anvil experiments.

II. EXPERIMENTAL METHODS

A. Multi-anvil apparatus

The multi-anvil experiments were conducted using both an in-house facility and synchrotron-based multi-anvil beamlines. The in-house experiments were performed using a 1500-ton multi-anvil press (DIA-1500T) equipped with an Osugi-type guide block,[21] installed at the Center for High Pressure Science and Technology Advanced Research (HPSTAR). The press employed six first-stage anvils made of 1.3395 steel (60–62 HRC) with 50 mm edge lengths at the anvil faces. The tetragonal compression asymmetry of the DIA-1500T press was calibrated using deformation of a steel dummy cube. The maximum dimensional difference among the three axes was within ±20 μm over a load range of 2.3–13.7 MN, significantly reducing the risk of blowout associated with asymmetric compression.

The *in situ* pressure calibrations were performed in a 2000-ton multi-anvil press with an Osugi-type guide block at the beamline BL12SW[22] of the Shanghai Synchrotron Radiation Facility (SSRF) and a six-axis multi-anvil press, Aster-15, installed at the beamline P61B[23] at the Deutsches Elektronen-Synchrotron (DESY). The press load in Aster-15 was converted to an equivalent uniaxial load in a multi-anvil press equipped with an Osugi-type guide block.

B. Assembly design and pressure determination

The 6–8 Kawai-type assembly composed of eight truncated cubic anvils, an octahedral pressure medium, and pyrophyllite gaskets was placed within a cubic compression space consisting of six first-stage anvils. In this study, two types of tungsten carbide cubes from Fujilloy Co., Ltd., TF05 and TJS01, with an edge length of 26 mm, were used as second-stage anvils, whose typical Vickers hardnesses are about HV2300 and HV2650, respectively. In some experiments, the anvils were machined with a 1° taper, while flat anvils were used in all the other experiments. All anvils were truncated to a TEL of 3 mm to compress a 7 mm edge-length octahedral pressure medium made of Cr_2O_3-doped MgO. The selection of binder-free TJS01 anvils and the implementation of anvil tapering were adopted based on the pioneering works for smaller assemblies (e.g., Kunimoto *et al.*,[15] Ishii *et al.*,[24] and Yamazaki *et al.*[13]).

Figures 1(a) and 1(b) present the cross section schematic diagrams of assemblies used for the in-house pressure calibration at HPSTAR. Pressure fixed points were determined by monitoring resistance changes associated with room-temperature phase transitions in ZnS (15.6 GPa[25]), GaP (23 GPa[26]), and Zr (34.5 GPa[27]). Regarding resistance measurement, GaP and ZnS were placed in the same MgO octahedron and separated by a Mo electrode [Fig. 1(a)], and the resistance was measured sequentially. The four-wire method was utilized in Zr resistance measurement [Fig. 1(b)]. The representative resistance curves are shown in Fig. 2.

Figure 1(c) illustrates the octahedral assemblies used at synchrotron-based multi-anvil beamlines. A pressure marker (MgO,[28] Fe,[29] or Mo,[30] see Table I) was placed adjacent to the sample. Pressures were estimated by measuring the unit cell volumes of the pressure markers and comparing them with their respective room-temperature equations of state (EOS). The energy-dispersive (ED-) XRD setups at beamline BL12SW and P61B were used to

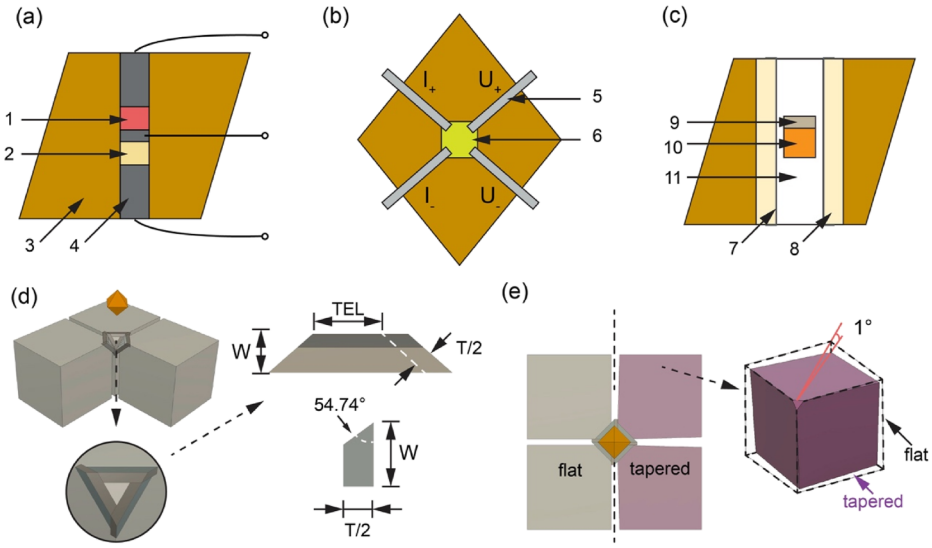

FIG. 1. Schematic diagrams of (a) the cross section of the *in situ* experiment assembly, (b) the pressure calibration assembly for semiconductor calibrants, (c) pressure calibration using the four-wire resistance method, and (d) the relative arrangement of the octahedral pressure medium, gaskets, and anvils. The enlarged view highlights the tapered gaskets attached to the anvil truncations, with the gasket dimensions indicated. (e) Comparison between flat and 1°-tapered anvils in top and side views. 1: GaP, 2: ZnS, 3: MgO pressure medium doped with 5 wt. % Cr_2O_3, 4: Mo electrode, 5: Pt foil electrode, 6: Zr, 7: Re foil heater, 8: thermal insulator, 9: pressure marker, 10: sample, and 11: spacer. TEL: truncated edge length of the second-stage anvil, T: thickness of the gasket, and W: gasket width measured from the truncation edge.

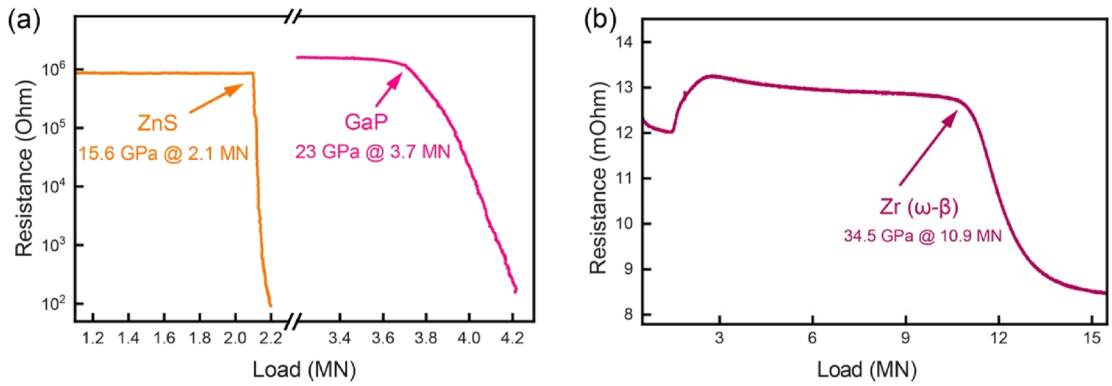

FIG. 2. Representative resistance measurements of (a) ZnS and GaP semiconductor calibrants and (b) the Zr metal calibrant.

measure the unit cell volumes of the pressure markers. A cylindrical rhenium foil heater (25 μm thick, ~1.7 mm in diameter) was used to heat the sample, and the temperature was measured using a type-D thermocouple inserted on the top of the sample. Various thermal insulation and spacer designs were employed depending on the sample materials and the targeted physical property measurements; these details are not relevant to the present study and will be reported elsewhere.

As illustrated in Fig. 1(d), in all experiments apart from run SK080, 24 identical pyrophyllite gaskets were glued around each anvil truncation; each of these gaskets was truncated at the front end, with an angle of 54.74° to the horizontal direction, to fit the gap between the anvils and the octahedron. The dimensions of the gasket were defined by TEL, width (W), and thickness (T). For the fixed TEL and OEL, T is geometrically constrained and can be calculated directly. The gasket widths (W) were set as 3, 2.67, and 2.5 mm in different experiments to investigate the effect of gasket volume on pressure generation. Before the experiments, all the gaskets were baked between 700 and 810 °C for 30 min. In run SK080, the conventional geometry gaskets (without truncation at the front end) were used, and the gasket width was 3 mm. To successfully mitigate blowout risks and ensure reproducible high-pressure generation, precise machining of the cell assembly and careful initial alignment of the first-stage anvils are paramount. As mentioned above, the tetragonal compression asymmetry was calibrated to be well within ±20 μm in our setup. While machining the tapered pyrophyllite gaskets requires slightly more preparation time compared to conventional flat designs, this precise geometric matching

TABLE I. Details of the experiments reported in this work.

Run No.[a]	Anvil material	Anvil geometry	Gasket geometry	V_gskt (mm^3)	Load at highest pressure (MN)	Highest pressure (GPa)	Pressure marker/calibrants
BT877	TJS01	1° tapered	W = 2.67 mm	386	11.9	45.8	Fe[29]
SK087	TF05	1° tapered	W = 2.5 mm	350	11.8	35.9	MgO[28]
DIA115	TF05	1° tapered	W = 2.5 mm	350	10.9	34.5	Zr[27]
DIA143	TF05	1° tapered	W = 2.5 mm	350	3.7	23	ZnS,[25] GaP[26]
SK017	TF05	1° tapered	W = 3.0 mm	460	12.7	30.7	MgO[28]
DIA015	TF05	1° tapered	W = 3.0 mm	460	4.7	23	ZnS,[25] GaP[26]
BT1044	TF05	Flat	W = 2.67 mm	386	8.0	32.7	Mo[30]
BT879	TF05	Flat	W = 2.67 mm	386	7.0	30.5	Fe[29]
SK080	TF05	Flat	Conventional	588	7.8	26.2	MgO[28]

[a]SK denotes the experiments done at the BL12SW beamline at SSRF, DIA denotes the experiments done using the DIA-1500T press at HPSTAR, and BT denotes the experiments done at the P61B beamline at DESY.

is an essential investment to minimize irregular deformation of the octahedron during the critical initial stages of compression.

III. RESULTS AND DISCUSSION

Experimental details are summarized in Table I. The assembly was first optimized by adjusting both the gasket volume and the second-stage anvil geometry (flat and 1° tapered anvils). Figure 3(a) shows the pressure generation results with varied gasket designs and anvil geometry configurations while employing the same type of second stage anvils (TF05, Fujilloy). The pressure generation efficiency of the conventional 7/3 assembly, which employs non-tapered gaskets with a width of 3 mm, is plotted for comparison. The results show that decreasing the gasket width [Fig. 1(d)], and thus reducing the gasket volume, plays a significant role in improving pressure generation efficiency, regardless of whether flat or tapered anvils are used. For example, experiments using optimized gaskets (W = 2.67 mm) and flat anvils (BT879, BT1044) generated pressures ~25% higher than those obtained with the conventional configuration at an applied press load of 7.8 MN (31.3 vs 24.9 GPa). This behavior likely reflects reduced lateral extrusion and plastic deformation of the gasket material, thereby limiting load dissipation outside the truncation-confined region, allowing the applied press load to be transferred more efficiently to the sample through the anvils. Previous studies[12,16,24] using smaller assemblies (TEL = 1.5 and 1.0 mm) suggested that tapering the anvil might compensate for the local deformation around the truncation and therefore, improve the pressure generation efficiency. However, our results indicated that the tapered anvils do not improve pressure generation efficiency when the 7/3 assemblies are used. As shown in Fig. 3(b), the pressures generated using flat and tapered anvils follow approximately the same trend with varying gasket volumes at 7.8 MN, with no significant difference observed. Nevertheless, the experiments using tapered anvils maintain higher efficiency at elevated loads and might ultimately achieve higher pressures under high-load conditions. For example, run SK087 with 1°-tapered anvils (TF05) and 2.5 mm-high gaskets reached 35.9 GPa at 11.8 MN, which is ~33% higher than the pressure reported in a previous study employing flat anvils and conventional gasket design under the same load (~27 GPa).[31] In addition, runs using tapered anvils maintained significantly wider anvil gaps than those using flat anvils under similar conditions, which is consistent with results from previous studies employing 1.5 mm TEL anvils.[13]

It is worth noting that results from in-house calibrations at HPSTAR and *in situ* pressure determination at the synchrotron beamline are in good agreement when identical assemblies are used. This consistency demonstrates both the good reproducibility of the assembly design and the comparability of experiments performed in the DIA-1500T press with those conducted at synchrotron beamlines (P61B at DESY and BL12SW at SSRF). The observed trends in pressure-generation efficiency are expected to be generally applicable to other Osugi-type multi-anvil systems. It has been suggested that reducing the gasket volumes will, in general, increase the risk of blowout under high pressure.[32] However, none of the experiments reported in Fig. 3 employing the optimized gasket configurations experienced gasket blowout or anvil failures even at the highest applied load, likely because optimized gasket geometries reported here represent a balance between pressure efficiency and mechanical stability, rather than an attempt to minimize gasket volume indefinitely.

Based on the empirical relationships identified in this study between gasket dimensions, anvil geometry, and pressure generation efficiency using TF05 anvils, we conducted an additional experiment (BT877) employing the optimized assembly together with harder WC anvils (TJS01, Fujilloy) to explore the pressure-generation capability of 3 mm TEL anvils. As shown in Fig. 4, experiments using the optimized assembly, featuring 2.67 mm-high gaskets and 1° anvil tapering—in combination with TJS01 anvils—exhibited a significant improvement in pressure generation efficiency across the entire applied load range (up to 11.9 MN) compared with previous studies, achieving a maximum pressure of 45.8 GPa at the highest load investigated. This pressure is ~70% higher than that achieved in conventional 7/3 experiments using TF05 anvils (~27 GPa)[12,31] and about 80% higher than those obtained using more conservative WC anvils (~25 GPa).[5] The optimized assembly design employed in the experiments in this study maintains higher pressure generation efficiency than previous studies using TJS01 WC anvils, producing pressures ~14% higher at the maximum load investigated in

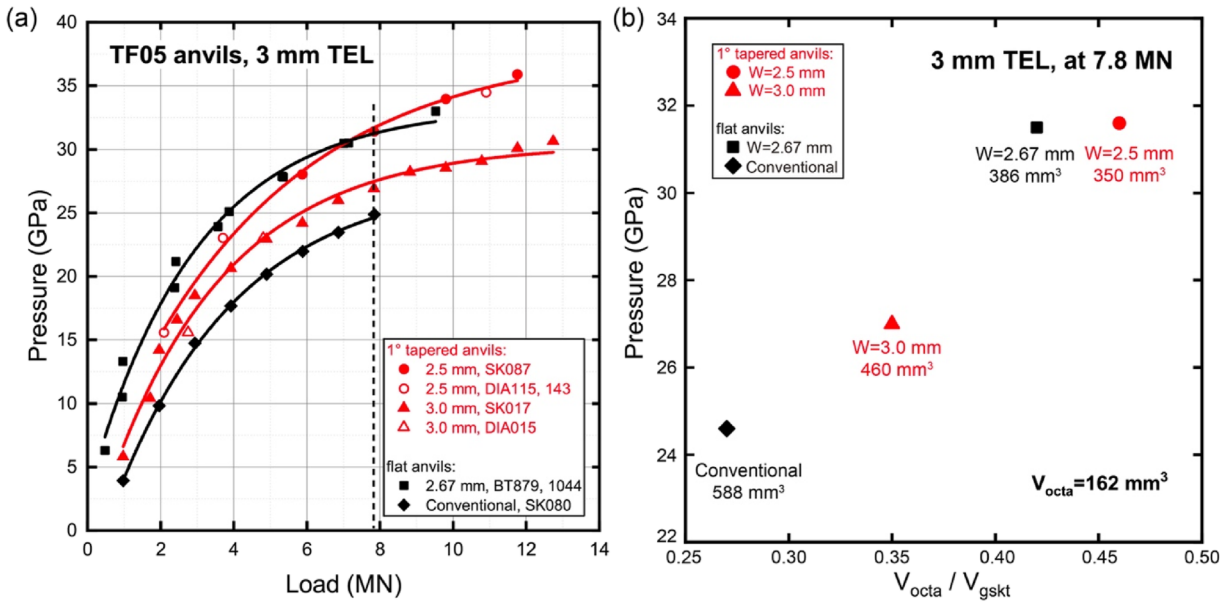

FIG. 3. Pressure generation efficiency dominated by gasket volume using TF05 flat anvils. (a) Results of pressure generation employing different gasket configurations (conventional, W = 2.5, 2.67, and 3.0 mm). (b) Comparison of the sample pressures at 7.8 MN as a function of octahedron-to-gasket volume ratio (V_{octa}/V_{gskt}).

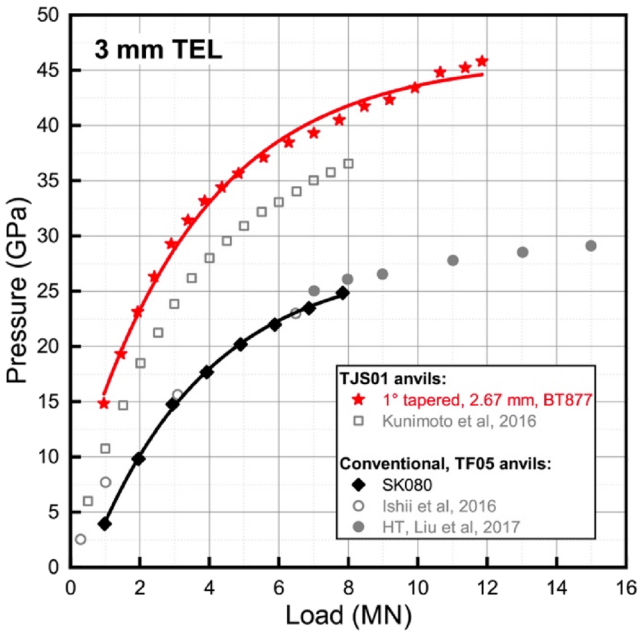

FIG. 4. Pressure generation curves of the optimized assembly using 3 mm TEL TJS01 anvils, compared with results from previous studies.

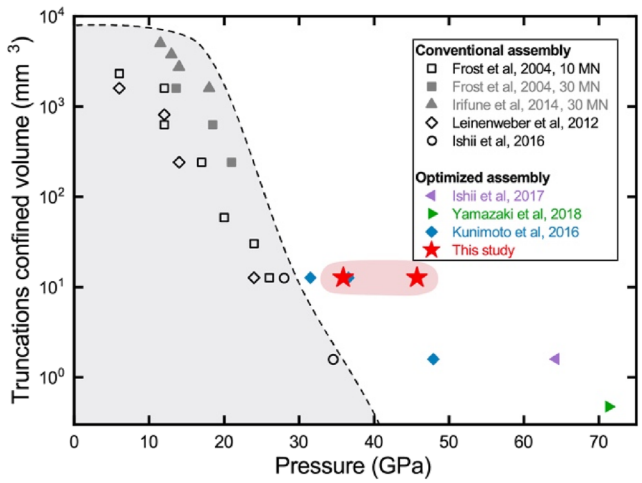

FIG. 5. Correlation between truncation-confined volume and pressure capability of multi-anvil techniques, employing WC anvils. Data for conventional assemblies are from Frost *et al.*,[34] Leinenweber *et al.*,[35] Irifune *et al.*,[36] and Ishii *et al.*[12] Data for optimized assemblies include results from Ishii *et al.*,[24] Yamazaki *et al.*,[13] and Kunimoto *et al.*[15]

that study (8 MN, 36 GPa)[15] and achieving a maximum pressure that is ~27% higher overall. Regarding decompression, experiments using conventional TF05 WC anvils showed no blowouts, allowing multiple reuses. In contrast, for all experiments employing TJS01 anvils, the anvils inevitably failed upon decompression. This failure is inherently due to the brittle nature of the nearly binder-free WC material, rather than a mechanical blowout during the compression cycle.

Figure 5 summarizes the correlation between sample volume and generated high pressures in the previous 6–8 multi-anvil studies, highlighting the inherent trade-off between achievable pressure

and sample volume. In the present study, we substantially extend the large-volume capability of multi-anvil techniques by achieving pressures of up to 45.8 GPa with TJS01 anvils and 35.9 GPa with TF05 anvils on truncation-confined volumes exceeding 10 mm^3, which is approximately an order of magnitude larger than the volumes accessible in previous studies that relied on 1.5 mm TEL anvils to reach comparable pressures. This advancement opens new possibilities for studying samples with large volumes under higher pressures; for example, this enables the synthesis and *ex situ* characterization of bulk novel materials above 40 GPa.[33] Furthermore, our optimized 3 mm TEL assembly exhibits significant potential for high-temperature applications (e.g., 2000–3000 K) since it has been well-established by previous studies at relatively lower pressures (e.g., Liu *et al.*[31]). Maintaining higher pressure at high temperatures relies on the delicate balance between thermal expansion and the softening-induced flow of the pressure medium. The substantially larger truncation-confined volume of our assembly can accommodate thicker thermal insulators (e.g., ZrO_2 or $LaCrO_3$) compared to smaller assemblies. This enhanced thermal insulation is expected to resist heat-induced flow more effectively, thereby minimizing the pressure drops often observed at extreme temperatures and preserving ultrahigh pressures for the synthesis of refractory materials.

In addition to substantially extending the achievable pressure range while maintaining a large sample volume, the optimized 7/3 assemblies exhibit good compatibility with *in situ* measurements by preserving wide anvil gaps at high pressures. As shown in the x-ray images in Figs. 6(a) and 6(b), the run BT877 with a 1°-tapered TJS01 assembly maintained a substantially larger anvil gap of 0.39 mm

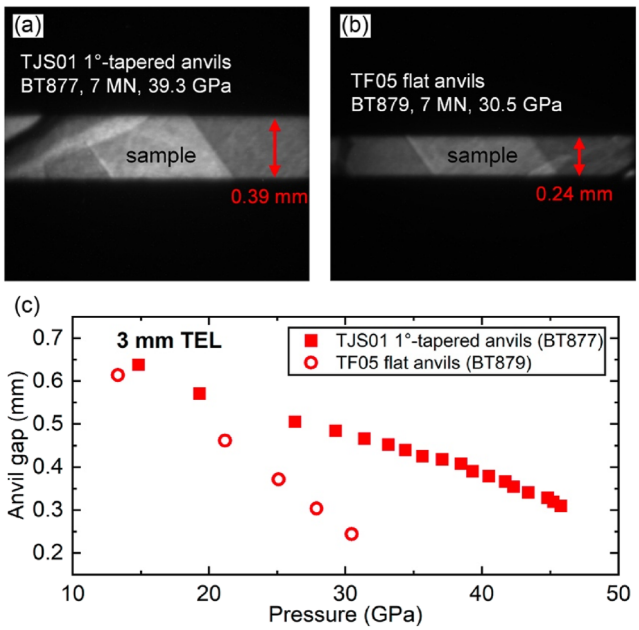

FIG. 6. Anvil gaps observed using tapered and flat anvils. (a) X-ray image of an experiment using 3 mm TEL TJS01 anvils with 1° tapering under 7 MN. (b) X-ray image using TF05 flat anvils under the same load. (c) Evolution of the anvil gap as a function of pressure.

while generating a pressure of 39.3 GPa at 7 MN. In contrast, the flat TF05 assembly compressed to a much narrower gap of 0.24 mm at the same load, generating a lower pressure of 30.5 GPa. Figure 6(c) systematically tracks the anvil gap evolution. The tapered geometry consistently preserves a wider opening throughout the compression cycle. This design is experimentally vital for *in situ* synchrotron-based experiments for the following reasons: a larger gap can (a) maximize the accessible angle for x-ray diffraction, which enables the acquisition of high-quality data with a shorter exposure time, and (b) facilitate x-ray imaging to obtain a more complete image of the sample, which is essential for determining wave travel distance in acoustic velocity measurements using ultrasonic interferometry. At pressures greater than 30 GPa, the experiments with flat anvils typically have a narrow anvil gap, which often precludes the utilization of these techniques.

The superior performance of the tapered anvils likely stems from their ability to compensate for anvil deformation under high applied loads. As illustrated in Fig. 7, under extreme loads, the WC anvils undergo significant elastic and plastic deformation, and the recovered anvils have a depression depth of ~50–70 μm near the anvil truncation. This deformation forms a "trumpet-like" opening, allowing the pyrophyllite gasket to extrude excessively. Furthermore, anvil deformation causes the adjacent anvil surfaces to become non-parallel, which substantially restricts x-ray access to the sample owing to the high x-ray opacity of WC. The 1° tapering [Fig. 7(b)] effectively pre-compensates for this elastic depression. By geometrically offsetting the anvil surface, the taper ensures that the truncation faces remain nearly parallel at high load.

By maintaining large sample volumes and wide anvil gaps at pressures exceeding 45 GPa, the technical developments presented in this study enable several physical property measurement techniques in multi-anvil presses to be extended to unprecedented pressure conditions. For example, ultrasonic interferometry in multi-anvil presses has long been limited to pressures below ~27 GPa[37] because large sample volumes are required to provide sufficiently long acoustic travel paths to resolve wave reflections at individual interfaces and to ensure precise distance measurements. Consequently, assemblies employing TELs smaller than 3 mm are impractical for such measurements. By applying the protocol developed in this study, acoustic velocity measurements using ultrasonic interferometry in a multi-anvil press can potentially be extended to pressures exceeding 45 GPa, corresponding to conditions of the mid-lower mantle. Such measurements will enable direct determination of the acoustic velocities of mantle minerals under relevant pressure–temperature conditions, facilitating meaningful comparisons with seismic observations and providing important constraints on the composition of Earth's deep interior. For electrical impedance and thermal conductivity measurements at high pressure, complex electrical circuits must be embedded within the multi-anvil assemblies, together with heating circuits for high-temperature generation. Consequently, large truncation-confined volumes are required to ensure the reliable operation of these circuits, which typically limits such measurements to assemblies employing TELs of 3 mm or larger (e.g., Ref. 38). For similar reasons as those underlying ultrasonic interferometry measurements, the technical developments presented in this study represent a prerequisite for extending electrical impedance and thermal conductivity measurements to higher pressure conditions. In addition, the larger anvil gaps achieved when

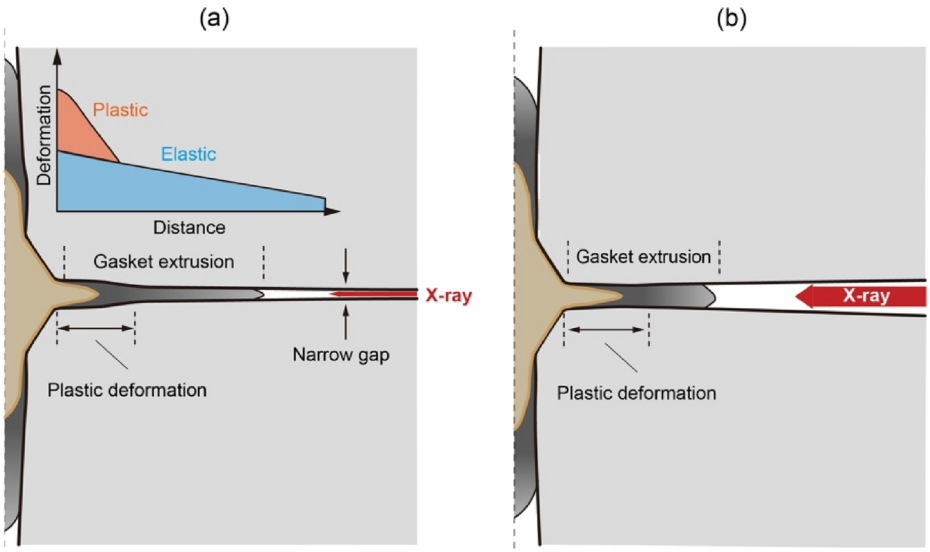

FIG. 7. Schematic cross sections of multi-anvil assemblies using (a) flat anvils and (b) tapered anvils. The insert in (a) illustrates the degree of deformation of the WC anvil with distance from the octahedral pressure medium.

employing tapered anvils facilitate the routing of electrical leads from the assembly through the anvil gaps to the exterior of the press, without short-circuiting against the WC anvils.

Moreover, this high efficiency in pressure generation enables the attainment of high sample pressure under reduced press load, thereby significantly mitigating the risk of mechanical failure due to overload, extending the fatigue life of the anvils. This ensures that routine operations at pressures above 30 GPa remain safe and sustainable for standard laboratory equipment. Unlike approaches that rely on expensive sintered diamond anvils, our strategy allows researchers to tailor the configuration according to specific scientific goals, balancing the anvil grade (e.g., TF05 vs TJS01) and gasket geometry. It should be noted that the present study focuses on room-temperature pressure generation; high-temperature performance will be addressed in future work. Furthermore, the optimization strategy developed here is also expected to be compatible with sintered diamond anvils, opening a pathway toward even higher pressures on millimeter-scale samples. From an economic perspective, our optimized gasket design allows for higher pressures at lower loads, thereby extending the fatigue life of conventional WC anvils. Since all eight corners of a flat anvil can be reused, this configuration is highly cost-effective for routine operations. Conversely, while TJS01 anvils are essential for reaching ultimate ultrahigh pressures, they currently cost significantly more and inevitably fail upon decompression due to their brittle nature. Therefore, the flexibility of our assembly design allows researchers in broader range of laboratories to balance the choice of anvil grade and experimental cost according to their specific scientific targets.

Looking forward, pushing the limits beyond 45 GPa over 10 mm^3 could be realized through several synergistic strategies: (1) further reducing gasket volume combined with advanced first-stage anvil alignment to maintain perfect cubic compression geometry; (2) exploring alternative gasket materials with superior mechanical properties; (3) systematically optimizing the anvil taper angle to better compensate for elastic deformation; and (4) utilizing larger WC anvils (e.g., 54 mm edge-length cubes) in higher-capacity presses to safely apply higher ultimate loads before reaching the anvils' mechanical limits.

IV. CONCLUSION

We have developed and evaluated an optimized 7/3 multi-anvil assembly utilizing WC anvils that achieves pressures of up to 45.8 GPa while maintaining a truncation-confined volume over 10 mm^3. By systematically optimizing the gasket geometry and anvil taper, we demonstrated that minimizing load dispersion and compensating for elastic deformation are critical for maximizing pressure-generation efficiency. This high-efficiency strategy enables the generation of extreme pressure conditions under moderate hydraulic press loads, thereby significantly extending the fatigue life of the anvils. As a result, routine laboratory operations for pressures higher than 30 GPa can become more economical, sustainable, and practical than approaches that push presses to their operational limits or employ expensive SD anvils.

The assembly is, therefore, well suited for the synthesis of bulk novel materials with millimeter-scale dimensions at pressures exceeding 45 GPa. Importantly, the optimized assembly preserves a wide anvil gap of ~0.3 mm even at peak pressures, ensuring compatibility with *in situ* diagnostic techniques, including x-ray imaging and diffraction at synchrotron-based multi-anvil beamlines. Moreover, the technical developments presented in this study satisfy a prerequisite for extending physical property measurements that require large sample volumes—such as ultrasonic, electrical impedance, and thermal conductivity measurements—to unprecedented pressure conditions in multi-anvil presses.

ACKNOWLEDGMENTS

H.G. acknowledges the support from the National Science Fund for Distinguished Young Scholars (Grant No. T2225027). We thank D. J. Frost for funding the TJS01 anvils used in the experiments. Y.L. was supported by the National Natural Science Foundation

of China (No. 12425403) and the National Key R&D Program of China (Grant No. 2021YFA1400300). We appreciate the thoughtful discussion with A. Wither, C. Liebske, and D. J. Frost. We acknowledge DESY (Hamburg, Germany), a member of the Helmholtz Association HGF, for the provision of experimental facilities. We thank S. Bhat and S. Sonntag for their assistance during the beamtime at P61B under Proposal Nos. I-20230775 and I-20241072. The beamline LVP instrument Aster-15 is funded by the ErUM-Pro program (Grant Nos. 05K16WC2 and 05K13WC2) of the German Federal Ministry of Education and Research (BMBF). We acknowledge the BL12SW beamline (http://cstr.cn/31124.02.SSRF.BL12SW) at the Shanghai Synchrotron Radiation Facility (SSRF), China, for the experimental support during approved beamtimes (Proposal Nos. 2024-SSRF-JJ-510860 and 2023-SSRF-JJ-505253).

AUTHOR DECLARATIONS

Conflict of Interest

The authors have no conflicts to disclose.

Author Contributions

Guoliang Niu and Lianjie Man contributed equally to this work.

Guoliang Niu: Conceptualization (equal); Formal analysis (equal); Investigation (equal); Methodology (equal); Writing – original draft (equal). **Lianjie Man**: Conceptualization (equal); Formal analysis (equal); Investigation (equal); Methodology (equal); Writing – original draft (equal). **Peiyang Mu**: Investigation (equal). **Junkai Li**: Investigation (equal). **Rémy Pierru**: Investigation (equal). **Amrita Chakraborti**: Investigation (equal). **Shuai Tang**: Investigation (equal). **Cheng Qian**: Investigation (equal). **Shengbo Cao**: Investigation (equal). **Shijing Zhao**: Investigation (equal). **Bingmin Yan**: Methodology (equal); Resources (equal). **Robert Farla**: Investigation (equal); Methodology (equal); Resources (equal). **Chunyin Zhou**: Investigation (equal); Methodology (equal); Resources (equal). **Xiaokang Feng**: Investigation (equal). **Youwen Long**: Funding acquisition (equal); Methodology (equal); Resources (equal). **Ke Yang**: Methodology (equal); Resources (equal). **Kui Han**: Investigation (equal); Methodology (equal). **Huiyang Gou**: Conceptualization (equal); Funding acquisition (equal); Project administration (equal); Supervision (equal); Writing – review & editing (equal).

DATA AVAILABILITY

The data that support the findings of this study are available from the corresponding author upon reasonable request.

REFERENCES

[1]N. Kawai and S. Endo, "The generation of ultrahigh hydrostatic pressures by a split sphere apparatus," Rev. Sci. Instrum. **41**, 1178 (1970).
[2]R. C. Liebermann, "Multi-anvil, high pressure apparatus: A half-century of development and progress," High Pressure Res. **31**, 493 (2011).
[3]P. F. McMillan, "New materials from high-pressure experiments," Nat. Mater. **1**, 19 (2002).
[4]T. Irifune, A. Kurio, S. Sakamoto, T. Inoue, and H. Sumiya, "Ultrahard polycrystalline diamond from graphite," Nature **421**, 599 (2003).
[5]H. Keppler and D. J. Frost, "Introduction to minerals under extreme conditions," in *Mineral Behaviour at Extreme Conditions*, edited by R. Miletich (European Mineralogical Union, Budapest, 2005), Vol. 7, pp. 1–30.
[6]E. Ito, "Multi-anvil cells and high-pressure experimental methods," in *Treatise on Geophysics*, 2nd ed. (Elsevier, 2015), Vol. 2, pp. 233–261.
[7]H. Marquardt and A. R. Thomson, "Experimental elasticity of Earth's deep mantle," Nat. Rev. Earth Environ. **1**, 455 (2020).
[8]S. I. Karato and D. Wang, "Electrical conductivity of minerals and rocks," in *Physics and Chemistry of the Deep Earth* (Wiley, 2013), Vol. 145.
[9]T. Katsura, "Thermal diffusivity of periclase at high temperatures and high pressures," Phys. Earth Planet. Inter. **101**, 73 (1997).
[10]L. Dubrovinsky, S. Khandarkhaeva, T. Fedotenko, D. Laniel, M. Bykov, C. Giacobbe, E. Lawrence Bright, P. Sedmak, S. Chariton, V. Prakapenka *et al.*, "Materials synthesis at terapascal static pressures," Nature **605**, 274 (2022).
[11]T. Boffa Ballaran, "Elasticity and composition of the earth's mantle," in *Structure and Dynamics of the Earth's Interior 2: Composition and Structure of the Earth's Mantle* (Wiley, 2025), Vol. 193.
[12]T. Ishii, L. Shi, R. Huang, N. Tsujino, D. Druzhbin, R. Myhill, Y. Li, L. Wang, T. Yamamoto, N. Miyajima, T. Kawazoe, N. Nishiyama, Y. Higo, Y. Tange, and T. Katsura, "Generation of pressures over 40 GPa using Kawai-type multi-anvil press with tungsten carbide anvils," Rev. Sci. Instrum. **87**, 024501 (2016).
[13]D. Yamazaki, E. Ito, T. Yoshino, N. Tsujino, A. Yoneda, H. Gomi, J. Vazhakuttiyakam, M. Sakurai, Y. Zhang, Y. Higo, and Y. Tange, "High-pressure generation in the Kawai-type multianvil apparatus equipped with tungsten-carbide anvils and sintered-diamond anvils, and x-ray observation on $CaSnO_3$ and $(Mg,Fe)SiO_3$," Comptes R. Géosci. **351**, 253 (2018).
[14]D. Yamazaki, E. Ito, T. Yoshino, N. Tsujino, A. Yoneda, X. Guo, F. Xu, Y. Higo, and K. Funakoshi, "Over 1 Mbar generation in the Kawai-type multianvil apparatus and its application to compression of $(Mg_{0.92}Fe_{0.08})SiO_3$ perovskite and stishovite," Phys. Earth Planet. Inter. **228**, 262 (2014).
[15]T. Kunimoto, T. Irifune, Y. Tange, and K. Wada, "Pressure generation to 50 GPa in Kawai-type multianvil apparatus using newly developed tungsten carbide anvils," High Pressure Res. **36**, 97 (2016).
[16]T. Ishii, Z. Liu, and T. Katsura, "A breakthrough in pressure generation by a Kawai-type multi-anvil apparatus with tungsten carbide anvils," Engineering **5**, 434 (2019).
[17]T. Kunimoto and T. Irifune, "Pressure generation to 125 GPa using a 6-8-2 type multianvil apparatus with nano-polycrystalline diamond anvils," J. Phys. Conf. Ser. **215**, 012190 (2010).
[18]X. Zhao, F. Ren, J. He, Y. Pan, H. Tang, X. Zhang, D. Yao, R. Liu, K. Hu, Z. Liu, and B. Liu, "Ultrahigh-pressure generation above 50 GPa in a Kawai-type large-volume press," Matter Radiat. Extremes **10**, 047801 (2025).
[19]T. Kunimoto, T. Irifune, and H. Sumiya, "Pressure generation in a 6-8-2 type multi-anvil system: A performance test for third-stage anvils with various diamonds," High Pressure Res. **28**, 237 (2008).
[20]B. Li, C. Ji, W. Yang, J. Wang, K. Yang, R. Xu, W. Liu, Z. Cai, J. Chen, and H. K. Mao, "Diamond anvil cell behavior up to 4 Mbar," Proc. Natl. Acad. Sci. U. S. A. **115**, 1713 (2018).
[21]J. Osugi, K. Shimizu, K. Inoue, and K. Yasunami, "A compact cubic anvil high pressure apparatus," Rev. Phys. Chem. Jpn. **34**, 1–6 (1964).
[22]K. Yang, Z.-H. Dong, C.-Y. Zhou, Z.-L. Zhao, D.-X. Liang, S.-C. Cao, and A.-G. Li, "Ultrahard X-ray multifunctional application beamline at the SSRF," Nucl. Sci. Tech. **35**, 98 (2024).
[23]R. Farla, S. Bhat, S. Sonntag, A. Chanyshev, S. Ma, T. Ishii, Z. Liu, A. Néri, N. Nishiyama, G. A. Faria, T. Wroblewski, H. Schulte-Schrepping, W. Drube, O. Seeck, and T. Katsura, "Extreme conditions research using the large-volume press at the P61B endstation, PETRA III," J. Synchrotron Radiat. **29**, 409 (2022).
[24]T. Ishii, D. Yamazaki, N. Tsujino, F. Xu, Z. Liu, T. Kawazoe, T. Yamamoto, D. Druzhbin, L. Wang, Y. Higo, Y. Tange, T. Yoshino, and T. Katsura, "Pressure generation to 65 GPa in a Kawai-type multi-anvil apparatus with tungsten carbide anvils," High Pressure Res. **37**, 507 (2017).
[25]G. J. Piermarini and S. Block, "Ultrahigh pressure diamond-anvil cell and several semiconductor phase transition pressures in relation to the fixed point pressure scale," Rev. Sci. Instrum. **46**, 973 (1975).

[26]S. Ono and T. Kikegawa, "Determination of the phase boundary of GaP using in situ high pressure and high-temperature x-ray diffraction," High Pressure Res. **37**, 28 (2017).
[27]Y. Tange, E. Takahashi, and K.-i. Funakoshi, "In situ observation of pressure-induced electrical resistance changes in zirconium: Pressure calibration points for the large volume press at 8 and 35 GPa," High Pressure Res. **31**, 413 (2011).
[28]Y. Tange, Y. Nishihara, and T. Tsuchiya, "Unified analyses for P-V-T equation of state of MgO: A solution for pressure-scale problems in high P-T experiments," J. Geophys. Res.: Solid Earth **114**, B03208, https://doi.org/10.1029/2008JB005813 (2009).
[29]P. I. Dorogokupets, A. M. Dymshits, K. D. Litasov, and T. S. Sokolova, "Thermodynamics and equations of state of iron to 350 GPa and 6000 K," Sci. Rep. **7**, 41863 (2017).
[30]X. Huang, F. Li, Q. Zhou, Y. Meng, K. D. Litasov, X. Wang, B. Liu, and T. Cui, "Thermal equation of state of molybdenum determined from in situ synchrotron X-ray diffraction with laser-heated diamond anvil cells," Sci. Rep. **6**, 19923 (2016).
[31]Z. Liu, M. Nishi, T. Ishii, H. Fei, N. Miyajima, T. B. Ballaran, H. Ohfuji, T. Sakai, L. Wang, S. Shcheka, T. Arimoto, Y. Tange, Y. Higo, T. Irifune, and T. Katsura, "Phase relations in the system $MgSiO_3$-Al_2O_3 up to 2300 K at lower mantle pressures," J. Geophys. Res.: Solid Earth **122**, 7775, https://doi.org/10.1002/2017jb014579 (2017).
[32]T. Irifune, H. Naka, T. Sanehira, T. Inoue, and K. Funakoshi, "In situ x-ray observations of phase transitions in $MgAl_2O_4$ spinel to 40 GPa using multianvil apparatus with sintered diamond anvils," Phys. Chem. Miner. **29**, 645 (2002).
[33]Z. Zeng, L. Yang, Q. Zeng, H. Lou, H. Sheng, J. Wen, D. J. Miller, Y. Meng, W. Yang, W. L. Mao, and H. K. Mao, "Synthesis of quenchable amorphous diamond," Nat. Commun. **8**, 322 (2017).
[34]D. J. Frost, B. T. Poe, R. G. Trønnes, C. Liebske, A. Duba, and D. C. Rubie, "A new large-volume multianvil system," Phys. Earth Planet. Inter. **143–144**, 507 (2004).
[35]K. D. Leinenweber, J. A. Tyburczy, T. G. Sharp, E. Soignard, T. Diedrich, W. B. Petuskey, Y. Wang, and J. L. Mosenfelder, "Cell assemblies for reproducible multi-anvil experiments (the COMPRES assemblies)," Am. Mineral. **97**, 353 (2012).
[36]T. Irifune, F. Isobe, and T. Shinmei, "A novel large-volume Kawai-type apparatus and its application to the synthesis of sintered bodies of nano-polycrystalline diamond," Phys. Earth Planet. Inter. **228**, 255 (2014).
[37]Y. Higo, T. Irifune, and K. I. Funakoshi, "Simultaneous high-pressure high-temperature elastic velocity measurement system up to 27 GPa and 1873 K using ultrasonic and synchrotron x-ray techniques," Rev. Sci. Instrum. **89**, 014501 (2018).
[38]T. Yoshino, S. Kamada, C. Zhao, E. Ohtani, and N. Hirao, "Electrical conductivity model of Al-bearing bridgmanite with implications for the electrical structure of the Earth's lower mantle," Earth Planet. Sci. Lett. **434**, 208 (2016).